Polymer Degradation and Stability 246 (2026) 111939

Contents lists available at ScienceDirect

Polymer Degradation and Stability

journal homepage: www.journals.elsevier.com/polymer-degradation-and-stability

High temperature performance of polyimide under accelerated thermal aging: linking chemical modifications to electrical properties

Jizhu Jin *, Davide Fabiani, Simone Vincenzo Suraci

Laboratory of Innovative Materials for Electrical Systems (LIMES), Department of Electrical, Electronic and Information Engineering (DEI), University of Bologna, Bologna (BO), Italy

ARTICLE INFO

Keywords:
Thermal aging
Polyimide
Condition monitoring
FTIR
Dielectric spectroscopy

ABSTRACT

Polyimide (PI) films are widely employed as high-temperature insulation in aerospace and electrical systems, where long-term reliability strongly depends on their thermo-oxidative stability. To evaluate their aging behavior, PMDA-ODA PI films were thermally aged in air at 280°C up to 60 days. Materials were tested by nondestructive techniques: Field Emission Scanning Electron Microscope (FE-SEM), Fourier Transform Infra-Red (FTIR) (using both ATR and transmission modes), dielectric spectroscopy, DC conductivity and thermally stimulated depolarization current (TSDC) measurements. The results reveal that the material remains stable during the first 10 days with limited oxidation. From 10 to 40 days, FTIR shows that oxidation gradually extends from the surface into the bulk, increasing the amount of carbonyl dipoles. This leads to stronger dipolar polarization, while microstructural rearrangements caused by chain scission enhance interfacial polarization and conductivity. In the later stage, both interfacial polarization and conductivity reach a stable plateau. DC conductivity and TSDC measurements jointly revealed a two-stage trap evolution: a pronounced reduction of activation energy and trap depth up to 30 days, followed by a slower stabilization phase. These findings deepen the understanding of polyimide aging and support the development of more reliable high-temperature insulation.

1. Introduction

During their application, aircraft and spacecraft materials are continually exposed to extreme environments that can deteriorate thermal, electrical, mechanical, and optical properties of their components. Among others, cables play a major role in terms of guaranteeing communication, control and safety of the equipment. For this reason, high-endurance materials are needed to be employed to ensure high reliability of the considered equipment.

Aromatic polyimides (PI) are high-performance materials prized for their excellent mechanical strength, chemical and thermal stability, and superior electrical insulation [1]. In particular, the high thermal stability of PI-based insulation systems makes them ideally suited for aerospace applications such as multilayer insulation systems, including multilayer thermal blankets (MLI), solar arrays, as well as for wiring insulation [2–4]. The wide applicability of such materials is also reflected by the big number of manufacturers providing this kind of materials with different formulations and functionalization additives.

Among the various degradation processes occurring during the aircraft's service life, thermal aging is both prevalent and particularly challenging for PIs. Although these materials are known for their excellent thermal stability, prolonged exposure to elevated temperatures can cause significant material aging and irreversible molecular damage. Aging leads to a deterioration or complete loss of material mechanical, insulating, and thermal barrier properties. These factors collectively pose a serious risk to cables and, in a larger view, to the aircraft reliability. Therefore, it is critical to understand the long-term structural changes that occur under thermal conditions, and which are the implication of such conditions for electrical functionality and reliability of PI-insulated wires in relative environments.

Numerous researchers have investigated the thermal aging of PI using various approaches. For instance, several studies have highlighted the strong temperature dependence of degradation kinetics, especially in the mid-temperature range (250–300°C) [5,6]. This temperature range coincides with the condition used in the present study (280°C), where both stabilization and degradation processes may co-exist. It highlights the need to dissect the competing mechanisms that govern the aging behavior. The work by Diaham's team and Ortelli et al. compared thermal aging in air and inert gas environments and identified oxygen as a critical factor in PI degradation [7,8]. Some studies have explored the

* Corresponding author.
E-mail address: jizhu.jin2@unibo.it (J. Jin).

https://doi.org/10.1016/j.polymdegradstab.2026.111939
Received 10 November 2025; Received in revised form 12 December 2025; Accepted 10 January 2026
Available online 11 January 2026

effects of thermal degradation on both the surface and the bulk of PI films with different thicknesses [9,10]. These results indicate that oxygen-driven degradation primarily affects the surface layer initially, potentially leading to different aging behaviors between the surface and the bulk of PI films.

Prior studies have identified oxidation, crosslinking, and chain scission as the main aging mechanisms, but the degree to which these molecular-scale changes dictate dielectric relaxation and charge transport dynamics remains insufficiently clarified [10]. These issues are particularly relevant in the 250–300°C regime. However, the interplay of the competing mechanisms in this temperature range remains insufficiently understood [5].

Most existing investigations have addressed only isolated aspects of PI degradation, such as surface oxidation kinetics or bulk structural changes, without systematically linking these processes to macroscopic electrical responses. For instance, surface-initiated oxidation and the subsequent formation of oxygen-limiting barrier layers have been reported [11], but how this progression into the bulk influences polarization phenomena and conduction pathways has not been quantitatively demonstrated. Unlike related studies on other thin-film dielectrics, the present work specifically targets PI films, examining the coupled evolution of surface-to-bulk oxidation and its direct implications for frequency- and temperature-dependent electrical behavior.

This work aims to clarify the coupled mechanism linking surface-to-bulk oxidation and trap evolution jointly shape the dielectric and conductive behavior of polyimide during long-term thermal aging. To achieve this, combined microstructural, chemical and electrical characterization, including FE-SEM, FTIR, dielectric spectroscopy, DC conductivity, and TSDC, were conducted to track oxidation growth and its influence on electrical performance. These insights deepen the understanding of oxidation and trap interactions governing polyimide degradation and provide a useful basis for improving the reliability of insulation in aerospace and other high-temperature applications.

2. Materials and methods

2.1. Materials and aging

Commercially available PI films were selected as test material in this study. Each specimen has a thickness of 55 ± 2 μm and a width of 10 cm. The PI used is synthesized from pyromellitic dianhydride (PMDA) and 4,4'-oxydianiline (ODA), corresponding to poly(pyromellitimide-1,4-diphenyl ether), which is chemically similar to DuPont's to Kapton® [12]. The detailed molecular structure is illustrated in Fig. 1.

To accelerate thermal aging, polyimide films measuring 10 × 12 cm were placed in a convection oven and exposed to air at 280°C for up to 60 days. To ensure uniform heat exposure, the specimens were suspended on a metal holder using clips, avoiding direct contact with the metallic racks of the oven that could otherwise lead to localized overheating. Samples were taken out at 10-day intervals to monitor the aging process. Including the unaged control, a total of seven film specimens were prepared for subsequent measurements. The overall procedure and setup are illustrated in Fig. 2 (a) and (b).

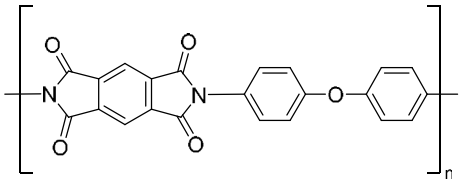

Fig. 1. Molecular structure of PMDA-ODA.

2.2. Experimental methods

2.2.1. Field emission scanning electron microscopy

Surface morphology was analyzed using a Field Emission Scanning Electron Microscope (FE-SEM, Tescan Mira3) operated at an accelerating voltage of 10 kV. Prior to imaging, all samples were metallized with a thin conductive coating to ensure optimal resolution. The magnification was adjusted to allow observation of surface features as small as approximately 1 μm, enabling detailed assessment of microvoids and crystal formation.

2.2.2. Fourier transformed infrared (FTIR) spectroscopy

The FTIR spectra were obtained using a PerkinElmer spectrometer in both attenuated total reflectance (ATR) mode and transmission mode. The ATR mode was employed to examine chemical changes at the material surface, with a typical penetration depth of 1–2 μm, while the transmission mode was used to probe the bulk chemical structure throughout the entire film thickness. The average scanning was conducted 16 times at the resolution of 4 cm^{-1} and spectral wavelength range of 4000–400 cm^{-1}. For the ATR mode, every sample was tested 3 times in different zones to consider possible inhomogeneities on chemical composition of the surface. Additionally, ATR-FTIR does not suffer from peak saturation, allowing for more detailed insights into the species formed on the surface. All the ATR spectra were normalized at 1496 cm^{-1}, corresponding to the C=C stretching vibration, which is commonly regarded as a chemically stable bond during the thermal aging of polyimide [9,13].

2.2.3. Dielectric spectroscopy

The dielectric measurements were conducted using a Novocontrol Alpha Dielectric Analyzer v2.2 with an applied voltage of 3 Vrms, a frequency ranged from 10^6 to 10^{-1} Hz and temperature variations of -50, 0, 20, 70, 120 and 150 °C. The analyzed frequency region enabled the investigation of both dipolar and interfacial polarization mechanisms occurring within the material, thereby highlighting the contribution of aging on polar species (e.g., oxidized chains) and microstructural modifications, respectively [11,14]. Frequencies below 0.1 Hz were not considered, since in this region the conductivity contribution dominates the dielectric loss factor, thereby obscuring the relaxation processes of interest. Moreover, the choice of different testing temperatures, on the one hand, allows the investigation of the dielectric properties at different operating temperatures and, on the other hand, it allows the investigation of relaxation mechanisms and derivation relative activation energy [15,16].

2.2.4. DC conductivity

The conductivity of the dielectric material can be derived by measuring the charging current based on standard ASTM D257-14 (2021) [17]. Prior to the measurements, the PI films were metallized by using a plasma cold sputtering setup to ensure good contact between the electrodes and insulation.

A Keithley 2290E-5 5kV was employed as HVDC generator and the charging current acquired by means of a picoammeter (Keysight B2981A). The conductivity (σ), was derived through the conduction current (i_{cond}), by using the following formula:

$$\sigma = \frac{J_c}{E} = \frac{i_{cond}/A}{E}(S/m) \quad (1)$$

where J_c represents the current density (A/m^2), E is the electric field which was set to 33 kV/mm in this study and A denotes the area of the measuring electrode, which has a diameter of 49 mm. All samples were measured at room temperature (~20 °C). In addition, unaged, 30- and 60-days aged samples were also tested at 70 °C and 120 °C, in order to track conductivity variations with aging under temperatures relevant to the intended applications.

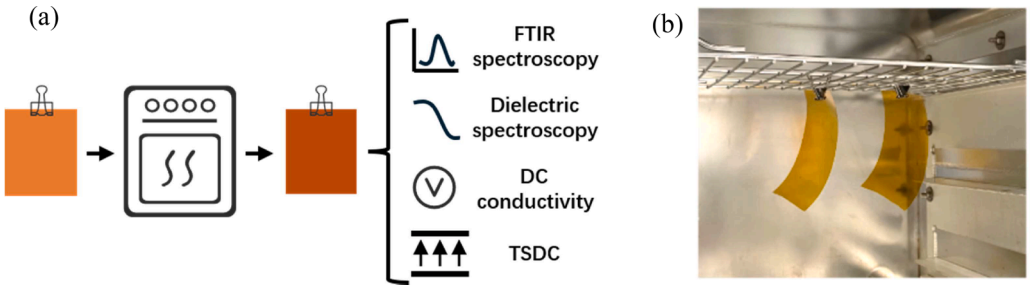

Fig. 2. (a) Schematic of the thermal aging and characterization process; (b) photograph of the oven setup with suspended PI film.

2.2.5. Thermally stimulated depolarization current (TSDC)

To investigate the trap distribution within the polymer during aging, TSDC analyses were carried out on PI films aged for 0, 30, and 60 days in order to investigate the evolution of trap states. The experiments were performed using a Novocontrol BDS1200 HV sample cell, with temperature precisely controlled by a Novocontrol Novocool system (liquid nitrogen cooling, accuracy ±0.1°C). A Keithley 2290E-5 (5 kV) served as the HVDC source, and the depolarization current was recorded with a Keysight B2981A picoammeter.

The experimental procedure comprised four main steps:

1. Polarization phase – The sample was polarized at $T_p = 70°C$ under a DC electric field of 33 kV/mm, consistent with the field conditions used in the DC conductivity tests and maintained until a steady conduction current regime was reached.
2. Cooling phase – The specimen was cooled down to $T_d = -50°C$ while keeping the electric field applied, thereby immobilizing the injected charges in traps.
3. Voltage-off stage – After stabilization at low temperature, the voltage was removed and the depolarization phase was prepared.
4. Depolarization and heating phase – The sample was subsequently heated at a constant rate of 3°C/min up to 150°C. During this stage, the thermally released carriers generated a depolarization current density J, which was continuously monitored.

This procedure enables the extraction of two fundamental parameters from the experimental data: (i) the evaluation of the main trap depth inside the material, and (ii) the determination of the trap distribution, i.e., the trap density as a function of trap depth. The calculation procedure of the trap distribution was carried out following the methodology reported in [18,19].

The choice of testing conditions was achieved by the analyses of different studies which report various polarization temperatures for TSDC tests on polyimide materials, with ~90°C being commonly adopted. In the present work, this temperature was initially considered; however, under the experimental conditions (high electric field >30 kV/mm, elevated temperature of 90°C, and relatively small sample size of 4 × 4 cm with ~55 μm thickness), significant surface currents were observed, causing the HVDC generator to shut down. To avoid this issue, a polarization temperature of 70°C was selected. According [20], tests performed at different polarization temperatures showed no substantial variation in peak positions between 50°C and 100°C under high electric fields. Based on this evidence, the chosen conditions (70°C and 33 kV/mm) are considered adequate to ensure space charge accumulation within the material bulk.

3. Experimental results

3.1. Optical microstructural observations

Fig. 3 shows SEM micrographs of PI samples: (a) unaged, (b) aged for 30 days, and (c) aged for 60 days.

The surface of the unaged sample (Fig. 3(a)) appears smooth and homogeneous, with only a few small dark spots, likely corresponding to microvoids inherent to the material. These minor inhomogeneities may result from handling during testing or slight imperfections introduced during manufacturing.

After 30 days of aging (Fig. 3(b)), the number of microvoids increases (highlighted by yellow arrows), and small crystals begin to form on the surface (see inset in Fig. 3(b)).

With longer aging (Fig. 3(c)), these changes become more pronounced. After 60 days, both the number and size of voids grow significantly, reaching approximately 4 μm in diameter (indicated by the red arrow), while surface crystal formation becomes extensive. These findings align well with previous observations reported by Zhang et al. [6] and can be attributed to thermo-oxidative degradation and chain scission processes, which promote localized stress relaxation and migration of low-molecular-weight species to the surface, facilitating crystal nucleation and growth, as it will be further detailed in the discussion section.

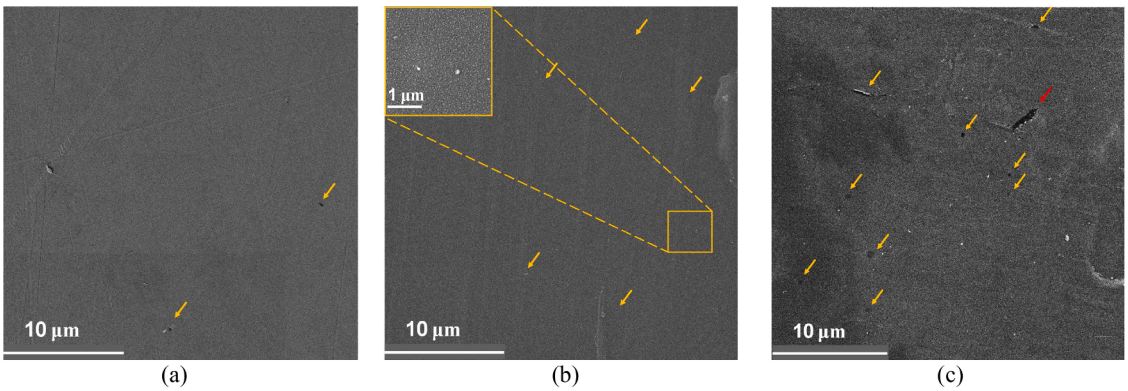

Fig. 3. FESEM micrographs of PI films at different aging times: (a) unaged, (b) 30 days, and (c) 60 days.

3.2. FTIR results

Fig. 4 presents the normalized FTIR spectra obtained under ATR mode for different thermal aging durations in the spectral range 2000–500 cm^{-1}, which includes key characteristic peaks [21]. Notably, no new peaks emerged throughout the aging process, indicating that no significant formation of new chemical species occurred. This observation suggests that the polyimide materials exhibit high chemical stability under the thermal aging conditions considered in this study. Table 1 reports the assignments of several peaks which are of interest for the aging analysis.

Previous studies on PMDA-ODA-based polyimides have demonstrated that the C-N bonds in this type of structure are particularly susceptible to degradation during thermal aging in air [6,8,22]. Under this aging condition, changes in the C=O bond also represent a critical feature to evaluate when assessing material degradation. In particular, the absorption bands at ~1775 cm^{-1} (in-phase vibration of C=O bond) and ~1712 cm^{-1} (out-of-phase vibration of C=O bond) were selected for analysis, as previous studies have reported their strong correlation with the structural evolution and oxidation of polyimide materials [9,13].

To investigate these structural changes in more detail, the peak intensities at 1712 cm^{-1}, corresponding to the out-of-phase vibrations of the C=O bond, and at 1370 cm^{-1}, attributed to the stretching vibration of the C-N bond, were selected for comparative analysis, as illustrated in Fig. 5. Both peaks exhibited a slight increasing trend.

Specifically, the C=O peak intensity increased gradually which indicate that the surface may react with oxygen in the air, leading to the formation of new carbonyl-containing groups such as carboxylic acid, ketones and aldehydes [6].

Moreover, an overall increasing trend is observed in the C-N peak intensity throughout the aging period. This phenomenon may be attributed to secondary imidization reactions of trace residual poly (amic acid) (PAA) segments present in the PI films. Literature has indicated that even commercially available polyimide films with a high degree of imidization (DOI) may retain small amounts of uncyclized PAA, particularly due to effects related to film thickness or rapid thermal processing [23,24]. Under the high-temperature aging condition (280°C), these residual PAA chains may undergo additional dehydration and cyclization, forming new imide rings and consequently enhancing the FTIR signal of the C-N bond.

While ATR-FTIR reveals chemical changes on the sample surface, the transmission mode offers additional insights into the bulk behavior of the material, overcoming limitations of ATR analysis. Observations from the transmission results indicate that most of the characteristic peaks show varying degrees of saturation. The only peak that remains suitable for analysis is located at 1775 cm^{-1} which corresponds to the imide C=O stretching vibration and is therefore considered in the following analysis. The results are presented in Fig. 6 and Fig. 7 as quantified peak areas. Fig. 6 illustrates the variation in the C=O absorption region, centered around the 1775 cm^{-1} peak, within the range of 1800–1762 cm^{-1}. Fig. 7 illustrates the variation in peak area values of the C=O bond, including error bars, over the thermal aging period. The relative stability observed in peak area values during the first 20 days of aging may derive from oxidation being largely restricted to the surface of the material,

Table 1
Characteristic FTIR absorption peaks and their vibrational assignments for polyimide.

Wavenumber (cm^{-1})	Vibrational Assignment
1775	In-phase vibration of C=O bond
1712	Out-of-phase vibration of C=O bond
1496	Aromatic C=C ring stretching
1370	Stretching vibration of C-N bond
1232	Asymmetrical stretching of C-O-C bond
1113	Imide C-N-C transverse stretching
721	Out-of-plane bending vibration of C-N-C bond

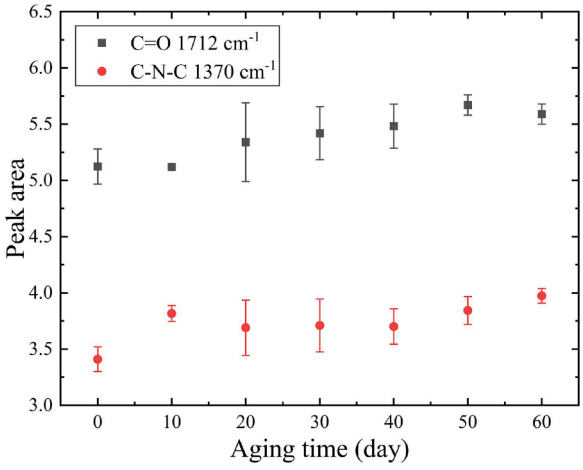

Fig. 5. Peak area variations of C=O (1712 cm^{-1}) and C-N (1370 cm^{-1}) in ATR-FTIR spectra of polyimide films during thermal aging.

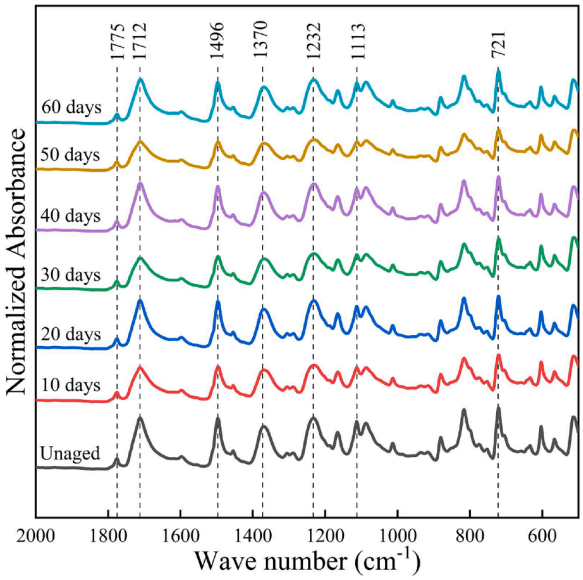

Fig. 4. FTIR spectra of ATR mode of PI films subjected to thermal aging.

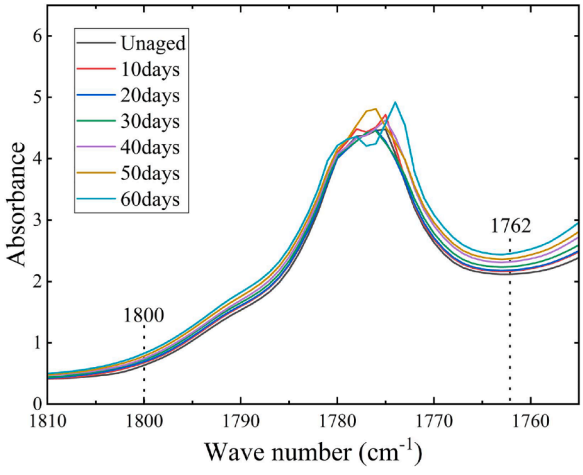

Fig. 6. Variation in the C=O absorption region centered around 1775 cm^{-1} (1800–1762 cm^{-1}) with aging time.

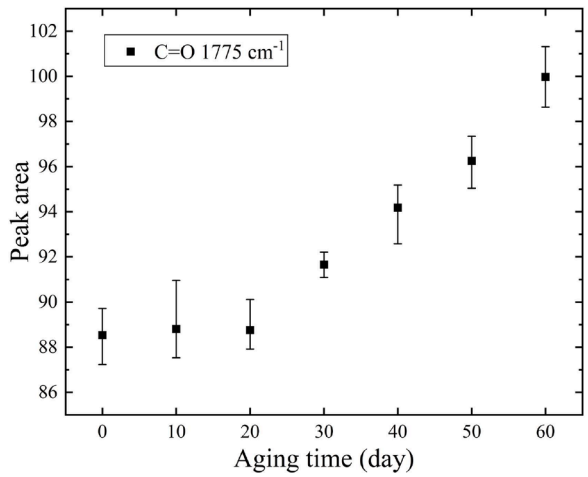

Fig. 7. Peak area values of the C=O absorption region with error bar over aging time.

hence not permeating in the bulk. This initial phase corresponds to an induction period in the thermo-oxidative degradation process, where oxygen diffusion into deeper layers is limited. After this transient, data show a consistent and gradual increase in peak area values, which is likely to signal the onset of more active and widespread oxidation beyond the surface layers.

3.3. Dielectric spectroscopy results

Fig. 8 reports the frequency-dependent dielectric response at room temperature (~20°C) for both the real part permittivity (ε′) and tanδ. In Fig. 8 (a), ε′ gradually increases with decreasing frequency. The unaged sample exhibits a relatively stable ε′ response over the entire frequency range, indicating a weak frequency dependence.

The real part of the permittivity exhibits a pronounced increase beginning at the initial aging interval of 10 days, suggesting an enhancement in the material's polarizability. This upward trend continues with prolonged aging, reaching a maximum around 40 days. Beyond this point, a decline in ε′ is observed. However, the value remains approximately 20% higher than that of the unaged reference sample, underscoring a sustained increase of permittivity despite the post-peak reduction. It is noteworthy that in the low frequency region below 10 Hz, the frequency dependence of ε′ is significantly stronger for the aged samples of 30 days and above, clearly differentiating them from the unaged and short-term aged samples and indicating enhanced interfacial polarization effects (Maxwell-Wagner-Sillars (MWS) polarization phenomenon) [25].

In the low-frequency region (approximately 100 Hz to 0.1 Hz), the tanδ-frequency profiles remain nearly unchanged during the first ten days of aging, indicating that early structural rearrangements have little influence on dielectric losses. After this period, a pronounced rise in tanδ is observed, accompanied by an increase in its slope with aging time. Anyway, the increase is not monotonic with aging, and a tentative structure-property analysis of the phenomenon will be illustrated in the discussion section.

In the high-frequency region (>1000 Hz), tanδ increases with frequency and shows a more consistent trend across the aged samples. A distinct relaxation peak, characteristic of the dipolar polarization [26,27], occurs between 10^5 Hz and 10^6 Hz, as seen in the insight plot shown in Fig. 8(c).

At the unaged state, this peak likely arises from the intrinsic dipolar properties of the polyimide backbone. The relaxation peak intensity slightly decreases within the first 10 days, followed by a gradual and nearly monotonic increase from 10 to 60 days. The overall variation remains modest up to 50 days, whereas a more pronounced rise appears at 60 days, where the relaxation becomes distinctly stronger.

To extend the room-temperature findings towards temperatures which may be characteristic of real-case scenarios, dielectric measurements were conducted across a range of temperatures to explore the thermal activation effects on ε′ and tanδ of unaged, 30 days and 60 days aged samples. As illustrated in Fig. 9(a, b and c), for samples with different aging times, the real part of permittivity generally follows a decreasing trend with increasing test temperature.

In the tanδ spectra, shown in Fig. 9(d, e and f), a distinct relaxation peak is observed at ~1000 Hz at –50°C. This peak shifts towards higher frequencies as the temperature increases, as expected. For temperatures higher than 70°C, the peak is moved outside the recordable frequency range. The recorded peak is seen in literature to be related to the γ local relaxation at low temperatures [16]. Based on the temperature dependence of the relaxation frequency, it is possible to derive the activation energy of the relaxation process in accordance to the formula:

$$\ln(f) = \ln(f_0) - \frac{E_a}{k_B T} \tag{2}$$

where f is the relaxation peak frequency, f_0 is the pre-exponential factor, E_a is the activation energy, k_B is the Boltzmann constant (8.617×10^{-5} eV) and T is the absolute temperature in Kelvin. Fig. 10 provides the Arrhenius plot of this relaxation frequency. The activation energy E_a is 0.44 eV, typical of the γ-relaxation process in polyimide [15,16].

3.4. DC conductivity results

Fig. 11 presents the evolution of the DC conductivity of PI films measured at room temperature as a function of aging time. Despite some

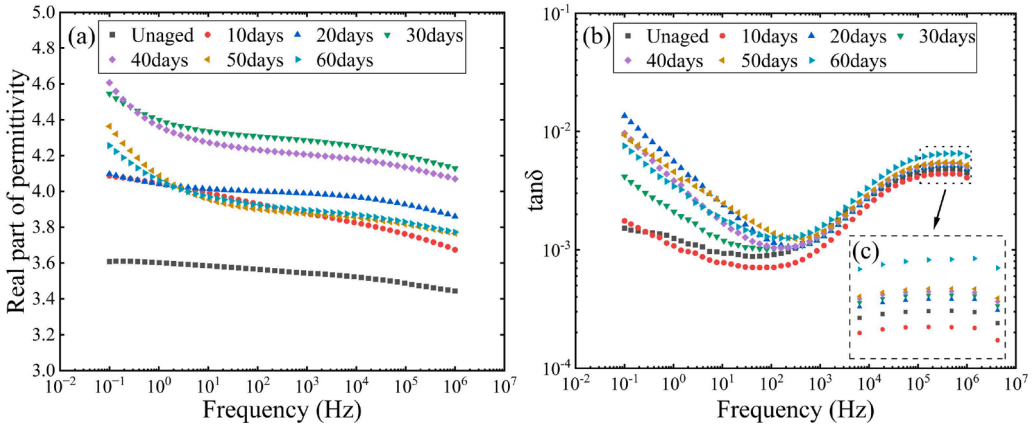

Fig. 8. (a) Real part of permittivity and (b) tanδ as a function of frequencies at room temperature; (c) insight of the high-frequency region (10^4–10^6 Hz) in (b).

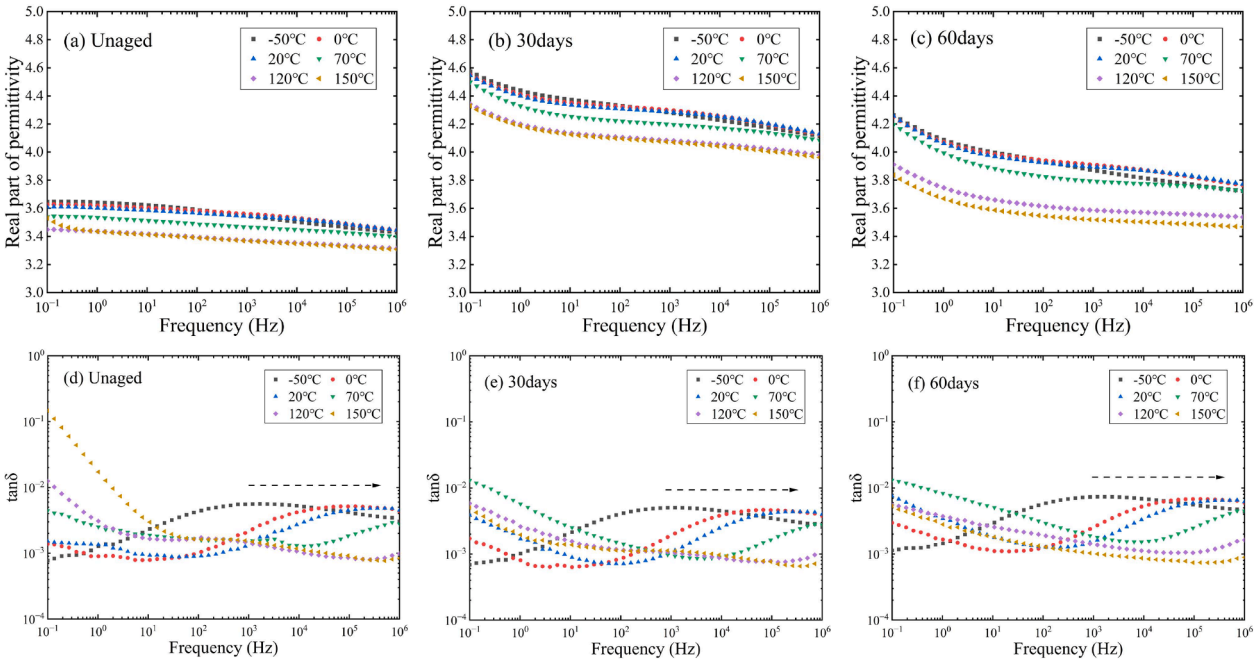

Fig. 9. The real part of permittivity (a, b and c) and tanδ (d, e and f) as functions of frequency at different temperatures for samples aged for 0, 30, and 60 days, respectively.

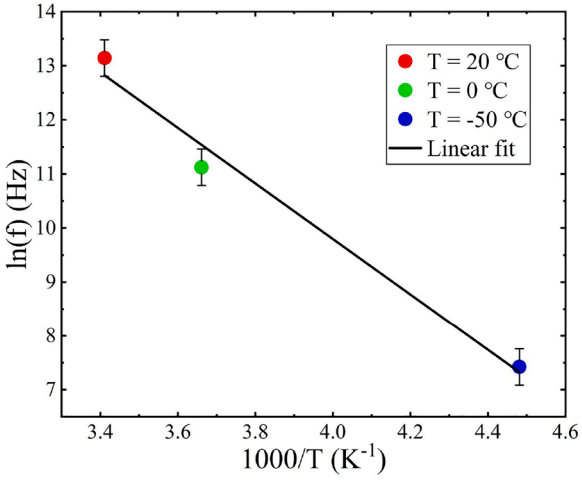

Fig. 10. Arrhenius plot of relaxation frequency with error bars.

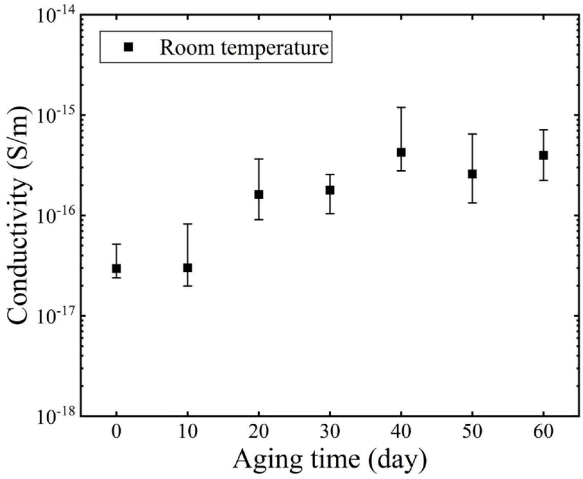

Fig. 11. DC conductivity at room temperatures.

fluctuations, the general trend demonstrates the increase of conductivity with thermal aging. During the first 10 days, the conductivity remains almost unchanged, suggesting that thermal aging has not yet significantly affected the electrical behavior of the material. This stability may be associated with the intrinsic thermal resistance of the imide backbone and the absence of extensive oxidation in the early stage.

Between 10 and 40 days, the conductivity rises markedly, reaching a peak at 40 days. At this point, the conductivity value is nearly 14 times greater than that recorded for the 10-day-aged sample, representing a change spanning more than one order of magnitude. This behavior is likely imputed to the buildup of new species e.g., oxidized groups or macromolecular rearrangement which may modify, in this case facilitate, the conduction mechanism within the polymer matrix. Beyond 40 days, conductivity shows only minor variations at 50 and 60 days, indicating a potential stabilization or plateau phase.

Fig. 12 shows the conductivity values as a function of testing temperature for unaged, 30 days and 60 days aged samples with error bars, measured at three different temperatures close to the typical operating conditions of the electrical equipment where PI is commonly used as insulating material in aerospace. With the increase in testing temperature, all three samples exhibit a monotonic rise, as expected. Also in this case, it is possible to plot the values of DC conductivity in an Arrhenius plot (Fig. 13), fitting is performed according to the following equation:

$$\ln(\sigma) = \ln(\sigma_0) - \frac{E_a}{k_B T} \tag{3}$$

where σ_0 is the pre-exponential factor and E_a is the activation energy for conduction. The values are shown in Table 2.

Interestingly, it is seen that the activation energy E_a is reduced from 0.53 eV to 0.26 eV (around 50%) in the first 30 days. This value changes very little in the later stages of aging, which can be more intuitively observed from the nearly parallel curves of the 30-day and 60-day samples in Fig. 13. This behavior likely stems from the distinct microstructural rearrangements occurring within the polymer matrix during the initial stages of aging, which appear to be preserved over time due to

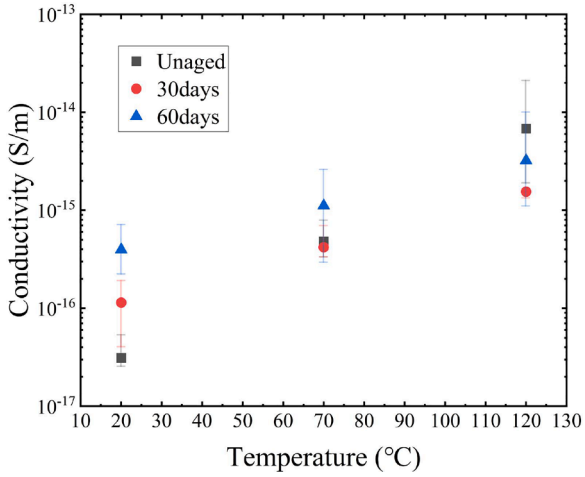

Fig. 12. DC conductivity at different testing temperatures with error bars.

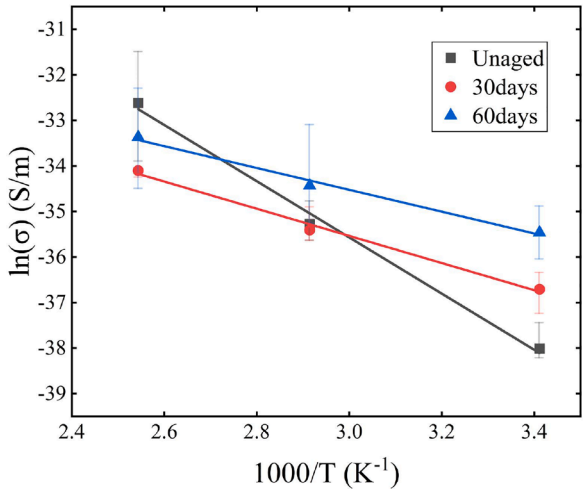

Fig. 13. Corresponding Arrhenius plot derived from DC conductivity measurements with error bars.

Table 2
Coefficients of Arrhenius Equations for DC conductivity.

Aging time (days)	Activation energy (eV)	σ_0 (S/m)
0	0.53	3.9272×10^{-08}
30	0.26	2.8426×10^{-12}
60	0.21	1.3491×10^{-12}

a training effect [28]. Additionally, the early aging phase may facilitate the gradual elimination of residual volatile compounds or weakly bound molecular fragments, contributing to a lowered energy barrier for charge transport and further influencing the material's long-term performance.

A lower activation energy in DC conductivity measurements is normally linked to the presence of shallower traps as seen in [29] and as it will be further discussed in the following.

3.5. TSDC results

Fig. 14 reports the smoothed depolarization current of unaged, 30-day, and 60-day aged PI films as a function of temperature. In TSDC measurements, various current peaks are recorded as the temperature increases, which are corresponding to the relaxation of dipolar species

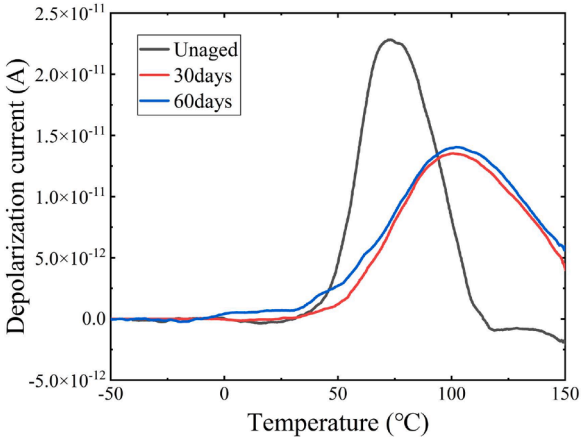

Fig. 14. Depolarization current curves of PI samples aged for 0, 30, and 60 days after smoothing.

and/or the gradual release (detrapping) of charges from trap centers.

Nonetheless, considering the very high electric field applied (33 kV/mm), it is reasonable to consider that the main current peaks are imputable to space charges within the polymer bulk.

The unaged sample exhibits a distinct current peak at approximately 70°C, whereas the peaks of the 30- and 60-day aged samples shift to nearly the same higher temperature of about 100°C. In addition, the current amplitude decreases by almost 50% compared with the unaged specimen, and the peak profiles become broader.

Subsequently, according to the calculation procedure reported in [18], the recorded current curves were processed and smoothed to obtain the corresponding trap distribution curves, as shown in Fig. 15. For the unaged specimen, the main trap peak is located at ~1.03 eV with a peak density of 1.0×10^{23} 1/(eV·m³). After 30 days of thermal aging, the trap depth decreases significantly to ~0.63 eV, while the density remains nearly unchanged. With further aging up to 60 days, the peak position shifts only slightly to ~0.41 eV, but the density increases (1.3×10^{23} 1/(eV·m³)).

It is worth noting that the temperature at which the peak occurs is only one of the parameters defining the trap depth, as the activation energy of the current density in an Arrhenius plot is the key parameter to consider for defining the trap depth. In this sense, it may happen that higher temperature peaks in the depolarization current do not always correspond to deeper traps, as also found in authors' previous works [19]. The used approach, called "initial rise method", was proposed by Bucci and Fieschi in [30] and recently reviewed by Song in [31]. This

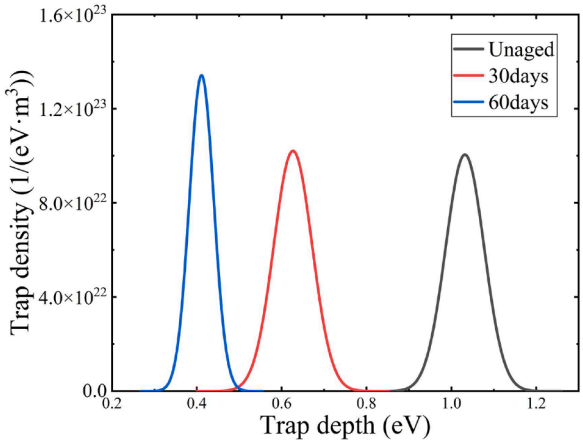

Fig. 15. Trap distribution curves of PI samples aged at 0, 30, and 60 days after smoothing.

method evaluates the slope of the Arrhenius plot (ln J vs 1/T) in the low-temperature region, which refers to the portion of the current–temperature curve before the peak, where the current starts to increase exponentially with temperature. This behavior guarantees that the release of charges is governed by a single activation energy and it reduces the impact of external factors, yielding more reliable and reproducible values for the trap depth, especially in complex dielectric systems.

4. Discussion

From the results reported in the previous Section, it is evident how accelerated thermal aging plays a significant role in the modification of the physical-chemical and electrical properties of PDMA-ODA. Indeed, despite its excellent thermal stability, the thermal aging temperature adopted in this work (280°C) is recognized as a critical regime where the aging behavior becomes highly complex, with stabilization and degradation processes occurring simultaneously and competing with each other [5].

Notably, the dominant aging mechanisms vary depending on the stage of exposure, leading to different observable effects. This behavior is expected, given the high thermal resistance of polyimides, which requires sufficient aging to trigger substantial degradation. Such mechanisms typically emerge only after the disruption of the polymer's main backbone, as it will be presented in the following. In order to ease the readability of the discussion section, it has been decided to divide into two main parts. The first focuses on the time-dependent evolution of the material properties, encompassing the early, mid-term, and long-term stages of oxidative thermal aging considered in this work, as summarized in Table 3. The second part examines the influence of testing and operating temperatures on the dielectric and conduction responses, highlighting how thermal activation and structural aging jointly affect the electrical behavior of polyimide films.

4.1. Time-dependent aging behavior of polyimide films

Table 3 summarizes the changes in key properties of the PI films as a function of aging duration, as discussed in the previous section. In particular, these properties were divided into two groups. The first one related to the effect of microstructural arrangements and the second one related to the oxidation build up within the polymer due to aging.

Microstructural arrangement can be likely associated to DC conductivity behavior due to (a) the contribution of conductivity in the tanδ value and (b) the predominance of the hopping conduction mechanism within the polymer chains. Likely, smaller chains created due to e.g., chain scission are characterized by higher charge mobility and enhance polymer conductivity, as confirmed by the agreement between the two parameters.

On the other hand, oxidation build up, verified by means of FTIR analyses, is associated with increase in dielectric losses within the dipolar polarization area due to the high electronegativity of oxygen which, once bonded with the PI reactive chains (e.g., after chain scission), leads to the formation of new species characterized by higher polarity and, consequently, the rise of the dipolar polarization response.

Table 3
Summary of the physicochemical and electrical property variations of PI films during thermal aging at 280°C in air.

Category	Parameter	Early (0–10d)	Mid-term (10–40d)	Long-term (40–60d)
Microstructural reorganization and conduction	Interfacial polarization peak	↔	↑↑	↔
	C–N groups (Surface)	↑↑	↔	↑
	Conductivity (σ)	↔	↑↑	↔
Oxidative progression	C=O groups (Surface)	↔	↑↑	↔
	C=O groups (Bulk)	↔	↑↑↑	↑↑↑
	Dipolar polarization peak	↓	↑	↑↑

[a] Note: The direction and extent of changes are indicated using the following symbols:
↑ slight increase; ↓ slight decrease;
↑↑ moderate increase; ↔ negligible change.
↑↑↑ pronounced increase;

4.1.1. Early aging (0–10 days)

In the initial stage of thermal exposure, oxidation appears to have a negligible impact on the polyimide insulation owing to the polyimide intrinsic thermal stability. As shown in Table 3, all parameters remain essentially stable except for the C-N bond and the dipolar polarization peak. The increase of the former is attributed to the secondary imidization process, as discussed earlier. Imidization in polyimides can be promoted by thermal aging, especially in the presence of residual polyamic acid groups or structural defects. The high temperatures involved in the aging process supply the energy needed to break C=O bonds, resulting in the formation of reactive intermediates such as free radicals or anhydride fragments. These species can then undergo recombination or rearrangement, forming more stable imide structures.

On the other hand, the slight decrease of the dipolar polarization peak may be likely related to either the physical loss of some polar species e.g., volatiles or mild crosslinking reactions occurring in the short aging period, as suggested by literature [13]. As a matter of fact, crosslinks hinder chain mobility, leading to a reduction of related relaxation mechanisms.

4.1.2. Mid-term aging (10–40 days)

After approximately ten days of exposure, FTIR results confirm that mild oxidation state is occurring in the material. Namely, the formation of new carbonyl-containing species (carboxylic acids, ketones, and aldehydes) occurs. In this framework, ATR-FTIR spectra display a progressive increase in the carbonyl absorption at 1712 cm^{-1} (Fig. 5), while transmission FTIR C=O band at 1775 cm^{-1} (Fig. 7) starts to rise markedly after ~20 days, confirming that oxidation initially develops at the surface and gradually extends into the bulk [6,21,32].

The enhancement of the dipolar polarization mechanisms due to oxidation [25] within the polymer matrix is reflected into the real part of permittivity and the dielectric losses at high frequencies (Fig. 8). In particular, the intensified dipolar polarization phenomenon is seen in literature to be possibly linked to the formation of low-molecular-weight polar species and free radicals in polyimide, including aromatic nitriles, aniline, toluidine, and hydroxyl groups introduced by moisture absorption [33].

In terms of polymer morphology, PMDA-ODA materials undergo significant modifications due to thermal aging. As an example, recent studies on thermal aging at 300°C of PMDA-ODA [34] report a sharp increase in crystallinity between 7 and 14 days. At the same time, literature provides evidence of chain scission [35] and subsequent crosslinking of fragmented chains [34]. In advanced aging stages, severe oxidation and embrittlement may also lead to the formation of microvoids and microcracks along with the formation of crystals on the material surface, as seen in SEM micrographs (Fig. 3(b)). All these processes may be considered as contributing causes of the increasing heterogeneity and interfacial effects in polymer morphology.

Thus, the marked rise in DC conductivity observed in Fig. 10 during this aging period may be attributed to two main factors: (i) an increase in the number of free charge carriers and (ii) enhanced mobility of shorter chains generated by chain scission. These combined effects facilitate free charge carrier accumulation at interfaces, intensifying Maxwell-Wagner-Sillars (MWS) polarization and amplifying the low-frequency

dielectric response (Fig. 8).

4.1.3. Long-time behavior (40–60 days)

After roughly 40 days of aging at 280°C, oxygen further penetrates and bulk oxidation accelerates, as evidenced by a gradual increase in the carbonyl peak area in transmission FTIR (Fig. 7), while the surface oxidation tends to reach a steady state (Fig. 5). The insulation oxidation level rises markedly, driving a pronounced growth in the amplitude of the high-frequency dipolar polarization peak (Fig. 8(b)).

The predominance of oxidative mechanisms reduces the microstructural modifications seen in the previous phases, likely due to the reaching of some sort of stability within the polymeric structure. Conductivity shows a constant behavior with aging, further confirming its correlation with the microstructural arrangement within the polymer matrix.

4.2. Temperature-dependent electrical behavior

Varying testing temperatures, the dielectric behavior of polyimide films is deeply modified. The dipolar polarization peak is seen to shift towards higher frequencies with increasing temperature. This is attributed to the local γ-relaxation process in polyimide, which involves restricted motion of chain segments such as side groups or rigid units [32]. The temperature dependence of this relaxation was further analyzed using an Arrhenius plot, yielding an activation energy of approximately 0.44 eV, consistent with literature values reported for secondary relaxations in polyimides [15,36]. It is worth noting that the relaxation peak frequency does not modify with aging, indicating that it originates from the dipolar response of the base polymer.

As PI materials are used for high temperature applications, the analysis of conductivity at different operating temperatures may demonstrate the suitability of these materials for field applications. As shown in Fig. 12 and 13, the temperature sensitivity of conductivity in aged samples is significantly reduced, evidenced by the decreasing slope of the conductivity–temperature curves and a notable reduction in activation energy by approximately 50%. In the later aging stage, it remains nearly unchanged from 30 to 60 days. This indicates that aging alters the fundamental conduction mechanism and the energy barrier distribution within the material. A lower E_a implies that charge carriers require less thermal energy to overcome migration barriers, facilitating easier transport. Previous studies [37] have suggested that chain scission and the formation of new intra-chain bonds may reduce the population of deep traps while increasing the density of shallow traps, thereby lowering the average activation energy. In such scenarios, charge carriers can be thermally activated with relatively low energy input.

This interpretation is further supported by the conductivity behavior at 120°C, where unaged samples exhibit higher conductivity than their aged counterparts. This behavior is likely imputed to the fact that, in the unaged state, conduction is dominated by deep traps, which require high activation energy, making the material more responsive to thermal excitation and leading to a sharper conductivity increase at elevated temperatures. In contrast, aged samples contain a greater number of shallow traps and polar transport pathways, enabling enhanced conduction at low temperatures but reducing the incremental effect of temperature, resulting in a more saturated response. This reasoning is further confirmed by TSDC trap analyses (Fig. 15) which confirm that between unaged and aged materials the main trap depth is almost halved.

5. Conclusions

This work provides a comprehensive understanding of the thermal aging behavior of PDMA-ODA polyimide at 280°C, revealing the complex interplay between stabilization and degradation processes that dictate its long-term performance.

The results highlight that aging induces both structural rearrangements and oxidative transformations, which evolve distinctly over time and collectively influence the dielectric and electrical properties of the material. The authors have proposed, according to the results shown, a three-stage ageing process involving structure-property relationships and reasoning related to the charge-transport mechanisms.

In the early aging stage, the polymer structure remains largely stable, with minimal oxidation and minor secondary imidization effects improving chain regularity. As exposure extends into the mid-term regime, oxidative processes become increasingly dominant, leading to the formation of carbonyl-containing species and low-molecular-weight polar fragments. After 40days, a stabilized microstructure governs the conduction mechanism within the polymer matrix.

Temperature-dependent measurements reveal that thermal activation significantly affects the dielectric and conduction mechanisms of aged samples. The observed reduction in activation energy and diminished temperature sensitivity of conductivity suggests a transition in the dominant charge transport process (from deep-trap to shallow-trap conduction) caused by chain scission and oxidation phenomena. Consequently, aged films exhibit enhanced low-temperature conduction but reduced response at elevated temperatures due to restricted molecular mobility and trap redistribution.

Overall, these findings help explain how structural stabilization and oxidative degradation interact in polyimides and provide useful guidelines for designing improved polymeric dielectrics. By showing how thermal aging affects electrical performance, this study contributes to the development of more reliable insulation materials for use in aerospace, electronics, and high-power electrical applications under extreme temperature conditions.

Building on the present study, future work will employ multi-temperature accelerated aging. This approach will allow a direct evaluation of the temperature dependence of degradation kinetics and strengthen predictive models for insulation performance under varying thermal conditions.

CRediT authorship contribution statement

Jizhu Jin: Writing – original draft, Investigation, Formal analysis, Data curation. **Davide Fabiani:** Writing – review & editing, Validation, Supervision, Investigation. **Simone Vincenzo Suraci:** Writing – review & editing, Visualization, Validation, Supervision, Project administration, Conceptualization.

Declaration of competing interest

The authors declare that they have no known competing financial interests or personal relationships that could have appeared to influence the work reported in this paper.

Acknowledgment

The project leading to this application has received funding from the National Recovery and Resilience Plan (NRRP), Mission 04 Component 2 Investment 1.5 – NextGenerationEU Award number: 0001052 and Euratom Research and Training Programme Award number: 101060008.

This publication reflects only the authors' view and the European Commission is not responsible for any use that may be made of the information it contains.

Data availability

Data will be made available on request.

References

[1] Z. Xu, Z.L. Croft, D. Guo, K. Cao, G. Liu, Recent development of polyimides: synthesis, processing, and application in gas separation, J. Polym. Sci. 59 (2021) 943–962, https://doi.org/10.1002/pol.20210001.

[2] P.R. Hondred, N. Bowler, M.R. Kessler, Electrothermal lifetime prediction of polyimide wire insulation with application to aircraft, J. Appl. Polym. Sci. 130 (2013) 1639–1644, https://doi.org/10.1002/app.39304.

[3] Y. Zhang, S. Dai, Z. Yin, W. Yan, Q. Li, H. Yuan, X. Zhang, L. Chen, J. Luo, X. Ouyang, B. Liao, W. Hao, J. Zhu, Integration fabrication of polyimide composite films for aerospace applications, SmartMat. 5 (2024) e1225, https://doi.org/10.1002/smm2.1225.

[4] S.V. Suraci, I. Benfridja, D. Fabiani, S. Diaham, Investigation of Si_3N_4 nanoparticles effect on the electrical properties of polyimide for power electronics applications, in: 2023 IEEE Conference on Electrical Insulation and Dielectric Phenomena (CEIDP), East Rutherford, NJ, USA, IEEE, 2023, pp. 1–4, https://doi.org/10.1109/CEIDP51414.2023.10410474.

[5] K. Rasmussen, G. Grampp, M.V. Eesbeek, T. Rohr, Thermal and UV degradation of polymer films studied in situ with esr spectroscopy, ACS Appl. Mater. Interfaces 2 (2010) 1879–1883, https://doi.org/10.1021/am100219z.

[6] L. Zhang, Y. Zhou, Y. Mo, Z. Zhou, Y. Sha, Z. Lu, Z. Cheng, Dielectric property and charge evolution behavior in thermally aged polyimide films, Polym. Degrad. Stab. 156 (2018) 292–300, https://doi.org/10.1016/j.polymdegradstab.2018.06.009.

[7] R. Khazaka, M.L. Locatelli, S. Diaham, P. Bidan, Effects of mechanical stresses, thickness and atmosphere on aging of polyimide thin films at high temperature, Polym. Degrad. Stab. 98 (2013) 361–367, https://doi.org/10.1016/j.polymdegradstab.2012.09.005.

[8] E.E. Ortelli, F. Geiger, T. Lippert, A. Wokaun, Pyrolysis of Kapton® in air: an *in situ* DRIFT study, Appl. Spectrosc. 55 (2001) 412–419, https://doi.org/10.1366/0003702011952163.

[9] R. Khazaka, M.L. Locatelli, S. Diaham, P. Bidan, Endurance of thin insulation polyimide films for high-temperature power module applications, IEEE Trans. Compon. Packag. Manuf. Technol. 3 (2013) 811–817, https://doi.org/10.1109/TCPMT.2013.2249559.

[10] J. Ahmad, M.G. Niasar, Aging behavior of PEEK, PTFE, and PI insulation materials under thermal oxidative and humid conditions for aerospace applications, J. Appl., Polym., Sci. 142 (2025) e56858, https://doi.org/10.1002/app.56858.

[11] S.V. Suraci, S. Amat, L. Hippolyte, A. Malechaux, D. Fabiani, C.Le Gall, O. Juan, N. Dupuy, Ageing evaluation of cable insulations subjected to radiation ageing: application of principal component analyses to Fourier transform infra-red and dielectric spectroscopy, High Volt. 7 (2022) 652–665, https://doi.org/10.1049/hve2.12239.

[12] J.E. Mark, Polymer data handbook, 2nd ed, Oxford University Press, New York, 2009.

[13] D. Sombel, M.-L. Locatelli, T. Lebey, Improvement of polyimide electrical properties during short-term of thermal aging, in: 2008 Annual report conference on electrical insulation and dielectric phenomena, 2008, pp. 79–82, https://doi.org/10.1109/CEIDP.2008.4772840.

[14] S.V. Suraci, D. Fabiani, A. Xu, S. Roland, X. Colin, Ageing assessment of XLPE LV cables for nuclear applications through physico-chemical and electrical measurements, IEEE Access. 8 (2020) 27086–27096, https://doi.org/10.1109/ACCESS.2020.2970833.

[15] R. Khazaka, M.L. Locatelli, S. Diaham, P. Bidan, L. Dupuy, G. Grosset, Broadband dielectric spectroscopy of BPDA/ODA polyimide films, J. Phys., D: Appl., Phys. 46 (2013) 065501, https://doi.org/10.1088/0022-3727/46/6/065501.

[16] S. Chisca, V.E. Musteata, I. Sava, M. Bruma, Dielectric behavior of some aromatic polyimide films, Eur., Polym., J. 47 (2011) 1186–1197, https://doi.org/10.1016/j.eurpolymj.2011.01.008.

[17] ASTM International, ASTM D257–14(2021): standard test methods for DC resistance or conductance of insulating materials. https://www.astm.org/d0257-14r21e01.html, 2021 accessed June 17, 2024.

[18] F. Tian, W. Bu, L. Shi, C. Yang, Y. Wang, Q. Lei, Theory of modified thermally stimulated current and direct determination of trap level distribution, J. Electrostat. 69 (2011) 7–10, https://doi.org/10.1016/j.elstat.2010.10.001.

[19] S.V. Suraci, D. Mariani, D. Fabiani, Impact of Antioxidants on DC and AC electrical Properties of XLPE-Based insulation systems, IEEE Access. 11 (2023) 76132–76141, https://doi.org/10.1109/ACCESS.2023.3297495.

[20] M.S. Gaur, R.K.Tiwari Ramlal, Study of trap structure of thermally polarized polyimide, J. Appl. Polym. Sci. 125 (2012) 520–526, https://doi.org/10.1002/app.35679.

[21] Y. Yang, D. Yin, R. Xiong, J. Shi, F. Tian, X. Wang, Q. Lei, Ftir and dielectric studies of electrical aging in polyimide under AC voltage, IEEE Trans., Dielectr., Electr., Insul. 19 (2012) 574–581, https://doi.org/10.1109/TDEI.2012.6180252.

[22] M. Tsukiji, W. Bitoh, J. Enomoto, Thermal degradation and endurance of polyimide films, in: IEEE International Symposium on Electrical Insulation, 1990, pp. 88–91, https://doi.org/10.1109/ELINSL.1990.109715.

[23] B.-H. Kim, H. Park, H. Park, D.C. Moon, Degree of imidization for polyimide films investigated by evolved gas analysis-mass spectrometry, Thermochim. Acta. 551 (2013) 184–190, https://doi.org/10.1016/j.tca.2012.10.029.

[24] W. Chen, W. Chen, B. Zhang, S. Yang, C. Liu, Thermal imidization process of polyimide film: interplay between solvent evaporation and imidization, Polymer 109 (2017) 205–215, https://doi.org/10.1016/j.polymer.2016.12.037.

[25] S.V. Suraci, C. Li, D. Fabiani, Dielectric spectroscopy as a condition monitoring technique for low-voltage cables: onsite aging assessment and sensitivity analyses, Energies 15 (2022) 1509, https://doi.org/10.3390/en15041509.

[26] S.V. Suraci, D. Fabiani, S. Roland, X. Colin, Multi scale aging assessment of low-voltage cables subjected to radio-chemical aging: towards an electrical diagnostic technique, Polym. Test. 103 (2021) 107352, https://doi.org/10.1016/j.polymertesting.2021.107352.

[27] E. Linde, L. Verardi, D. Fabiani, U.W. Gedde, Dielectric spectroscopy as a condition monitoring technique for cable insulation based on crosslinked polyethylene, Polym. Test. 44 (2015) 135–142, https://doi.org/10.1016/j.polymertesting.2015.04.004.

[28] S. Guénon, S. Scharinger, S. Wang, J.G. Ramírez, D. Koelle, R. Kleiner, I.K. Schuller, Electrical breakdown in a V2O3 device at the insulator-to-metal transition, EPL 101 (2013) 57003, https://doi.org/10.1209/0295-5075/101/57003.

[29] L.A. Dissado, G.C. Montanari, D. Fabiani, Fast soliton-like charge pulses in insulating polymers, J. Appl. Phys. 109 (2011) 064104, https://doi.org/10.1063/1.3554694.

[30] C. Bucci, R. Fieschi, G. Guidi, Ionic thermocurrents in dielectrics, Phys., Rev. 148 (1966) 816–823, https://doi.org/10.1103/PhysRev.148.816.

[31] H. Song, J.P. Goud, J. Ye, W. Jung, J. Ji, J. Ryu, Review of the thermally stimulated depolarization current (TSDC) technique for characterizing dielectric materials, J. Korean Ceram, Soc. 60 (2023) 747–759, https://doi.org/10.1007/s43207-023-00305-5.

[32] L. Li, N. Bowler, P.R. Hondred, M.R. Kessler, Influence of thermal degradation and saline exposure on dielectric permittivity of polyimide, J. Phys. Chem. Solid. 72 (2011) 875–881, https://doi.org/10.1016/j.jpcs.2011.04.004.

[33] R. Torrecillas, A. Baudry, J. Dufay, B. Mortaigne, Thermal degradation of high performance polymers—influence of structure on polyimide thermostability, Polym., Degrad, Stab. 54 (1996) 267–274, https://doi.org/10.1016/S0141-3910(96)00052-3.

[34] S. Marin, M. Yacouti, M. Shakiba, Thermo-oxidative aging of semi-crystalline polyimide films: experimental characterization and predictive modeling, Polym. Degrad. Stab. 243 (2026) 111714, https://doi.org/10.1016/j.polymdegradstab.2025.111714.

[35] J. Wu, A. Miyahara, A.R. Khan, M. Iwata, K. Toyoda, M. Cho, X.Q. Zheng, Effects of ultraviolet irradiation and atomic oxygen erosion on total electron emission yield of polyimide, IEEE Trans., Plasma Sci. 42 (2014) 191–198, https://doi.org/10.1109/TPS.2013.2288699.

[36] S.Z.D. Cheng, T.M. Chalmers, Y. Gu, Y. Yoon, F.W. Harris, J. Cheng, M. Fone, J. L. Koenig, Relaxation processes and molecular motion in a new semicrystalline polyimide, Macromol. Chem. Phys. 196 (1995) 1439–1451, https://doi.org/10.1002/macp.1995.021960507.

[37] V. Henri, E. Dantras, C. Lacabanne, F. Koliatene, C. Trebosc, Ageing of polyimide under thermal stress: relaxational effects and charge transport, Polym., Degrad., Stab. 186 (2021) 109524, https://doi.org/10.1016/j.polymdegradstab.2021.109524.